# Improvements to the Johnson noise thermometry system for measurements at 505 - 800 K

K. Yamazawa, W. L. Tew, A. Pollarolo, H. Rogalla, P. D. Dresselhaus, and S. P. Benz

Citation: AIP Conference Proceedings **1552**, 50 (2013); doi: 10.1063/1.4819514
View online: http://dx.doi.org/10.1063/1.4819514
View Table of Contents: http://scitation.aip.org/content/aip/proceeding/aipcp/1552?ver=pdfcov
Published by the AIP Publishing

# Improvements to the Johnson Noise Thermometry System for Measurements at 505 – 800 K

K. Yamazawa[1,3], W. L. Tew[1], A. Pollarolo[2], H. Rogalla[1], P. D. Dresselhaus[2] and S. P. Benz[2]

[1] *National Institute of Standards and Technology, Gaithersburg, MD, USA*
[2] *National Institute of Standards and Technology, Boulder, CO, USA*
[3] *National Metrology Institute of Japan, AIST, Tsukuba, Ibaraki, Japan*

**Abstract.** We report new results for Johnson noise thermometry in the range 693 K to 800 K. The results are based on operation of a quantized voltage noise source (QVNS) which serves as a reference for the relative noise power spectral density. This paper describes the modifications to the system in order to overcome the limitations in our previous work and furthermore enable measurements of $T$-$T_{90}$ at higher temperatures.

**Keywords:** Johnson Noise Thermometry, Thermodynamic temperature measurement, Quantized Voltage Noise Source.

## INTRODUCTION

The resolution at the 24th meeting of the General Conference on Weights and Measures (CGPM), upon the possible future revision of the International System of units (SI) states that the kelvin will continue to be the unit of thermodynamic temperature, but its magnitude will be set by fixing the numerical value of the Boltzmann constant [1]. This significant change gives importance to projects determining the Boltzmann constant based on the current definition, as well as those determining the deviations at various temperatures between the thermodynamic temperature and the ITS-90 temperature scale. This information is compiled and reviewed by the Working Group 4 of the Consultative Committee for Thermometry (CCT-WG4) [2,3]. To avoid systematic errors specific to the measurement method, it is very important to have multiple thermodynamic techniques available in overlapping ranges of temperature to support the foundation of the temperature scale.

The National Institute of Standards and Technology (NIST) is currently using Johnson noise thermometry (JNT) to determine the deviations of the International Temperature Scale of 1990 (ITS-90) from the thermodynamic temperature in the range of 505K–933 K, overlapping the ranges of both acoustic gas-based and radiation-based thermometry. The JNT system utilizes a quantized voltage noise source (QVNS) as a reference for the noise power spectrum. This paper describes the modifications to the system as a challenge to overcome the limitations in our previous work [4-7] and furthermore enable measurements at higher temperatures. We built two types of resistance probes designed for higher temperatures and modified the amplifiers to achieve lower distortion [8]. Results of our measurements from 505 K up to 800 K and the possible future improvements learnt through this activity are presented in this paper.

## THE QVNS BASED JNT SYSTEM

JNT is a method to measure the thermodynamic temperature $T$ by measuring the power spectral density $S_R$ of the thermal noise generated within a conductor with resistance $R$. The Nyquist equation [9,10]

$$S_R = 4kTR \tag{1}$$

is known to be a valid approximation to within $1\times10^{-6}$. Since the noise voltage spectral density is as small as 1.73 nV·Hz $^{-1/2}$ for a 107 Ω resistor at 505 K, the noise signal is amplified with two identical amplification systems and the cross correlation is taken to measure the noise power. The stability of the amplification is another engineering challenge requiring cancelation of any time dependent drift of the amplifiers through switching of the input between the reference noise source with a known spectral density and the unknown thermal source.

In our system, we calculate the cross correlation in frequency domain by digitizing and performing Fast Fourier Transformations (FFTs). For the reference, apart from the conventional method employing another resistor probe placed into a known temperature as the reference, NIST employs a quantum-based approach. The quantized voltage noise source (QVNS) is an application of Josephson junctions (JJs) to generate a pseudo-noise waveform with a calculable

*Temperature: Its Measurement and Control in Science and Industry, Volume 8*
AIP Conf. Proc. 1552, 50-55 (2013); doi: 10.1063/1.4819514
2013 AIP Publishing LLC 978-0-7354-1178-4/$30.00

noise density. A harmonic series of sine waves with the same amplitude matching the thermal source's power spectral density, but with a random phase for every harmonic, is used as the pseudo-noise waveform. A pulse bit stream is generated from a delta-sigma conversion of this waveform which, in conjunction with its complement, drives two series arrays of JJs. A 1 $cm^2$ chip with 20 superconductor-normal metal-superconductor (SNS) JJs driven by a special self-biasing method [11,12] is employed in our experiment. The chip is held within a shielded probe (JJ-probe) which is immersed in liquid He within a 100 liter dewar.

The basic structure of the JNT system used in this experiment is described elsewhere [7]. A vacuum furnace with 4 thermo wells accommodates the JNT resistor probe and a standard platinum resistance thermometer (SPRT) calibrated to the ITS-90 for the comparison measurement. The QVNS generates a pseudo noise with a power spectral density closely matched to that of the resistor within the furnace. The two noise sources, thermal and quantized, are measured in turn with the cross correlator and recorded on the computer. Through the data analysis and comparison of the noise power, we can determine the thermodynamic temperature in absolute mode [7],

$$T = \left\langle \frac{S_{\mathrm{R}}}{S_{\mathrm{J}}} \right\rangle \Bigg|_{f=0} \frac{S_{\mathrm{J\text{-}calc}}}{4kR} \tag{2}$$

or in relative mode

$$\frac{T_2}{T_1} = \left\langle \frac{S_{\mathrm{R2}}}{S_{\mathrm{J2}}} \right\rangle \left\langle \frac{S_{\mathrm{J1}}}{S_{\mathrm{R1}}} \right\rangle \Bigg|_{f=0} \frac{S_{\mathrm{J2-calc}}}{S_{\mathrm{J1-calc}}} \frac{R_1}{R_2} \tag{3}$$

from measurement results at two different furnace temperatures, $T_1$ and $T_2$. $S_{\mathrm{R}}$ and $S_{\mathrm{J}}$ are the measured spectral power densities of the resistor and JJs, and $S_{\mathrm{J\text{-}calc}}$ is the calculated spectral power density of the pseudo noise. The frequency data are binned around the QVNS tones [9,10] to calculate the ratio.

The furnace temperature is controlled by a digital PID controller and the stability is typically around ± 1 mK at 505 K, and the stability slightly degrades at higher temperatures. Upon combining various data sets of measurements performed at the same temperature, the ratio data was normalized by using the following equations before calculating the thermodynamic temperatures using either equation (2) or (3).

$$\left\langle \frac{S'_R}{S'_J} \right\rangle = \left\langle \frac{S_{\mathrm{R}}}{S_{\mathrm{J}}} \right\rangle - X_{90} + 1 \tag{4}$$

where $X_{90} \equiv 4kT_{90}R(T_{90})/S_{\mathrm{J\text{-}calc}}$.

# MODIFICATIONS TO THE SYSTEM

## JNT resistor probes

The JNT resistor probe is an adaptation of conventional immersion-type resistance thermometers. To enable stable measurements of the noise generated at the resistors, we adopted a design as shown in Fig 1. Two resistor elements are wired to the grounding point to determine the electrical potential of the probe and enable dc coupling to the differential amplifiers. The wiring to the two differential inputs, channels A and B, are independently wired at the stem. The resistors are made from Pt-W (8%) filaments that exhibit a moderately low temperature coefficient of resistance (~300 μΩ/Ω·K) and sufficient stability at the temperatures for our measurements. To further assure stability, we placed the probe structure within a clean quartz sheath with a gas tight head and purged the container with pure Ar gas to avoid oxidation of the sensing elements. Gold wire with 0.25 mm diameter was used for the stem wiring.

The stem structure has two functions; as the transmission line conveying the noise signal, and as the section of the probe that maintains the temperature gradient between the measurement and room temperatures. For this work, we designed two probes with different stem structures as shown in Fig. 2.

Probe JNT-9 uses the same two bore synthetic quartz material with a square cross section and low $OH^-$ content as used in our previous work [4-7]. In order to increase the cancelation of EMI-induced voltages in the leads, the stem structure was divided into 8 unit segments with a ¼-twist in each. Quartz disks hold the leads for the two channels in place between the unit segments. The capacitance between the two leads for each channel is approximately 12 pF. The sheath outer diameter for this probe is 11 mm.

Since the capacitance between the leads will act as a low pass filter to the noise signal, it is preferable to have a lower capacitance. We designed the JNT-10 probe with this in mind. As shown in Fig. 2(b), it has a similar structure to the stem of an ordinary SPRT, and the additional 5th wire for the GND connection is threaded through the center hole. By adoption of this design, we were able to reduce the outer diameter of the sheath to 7 mm and to decrease the capacitance between the lead wires to approximately 6 pF. Despite this modification, there was no obvious additional EMI pickup compared to that of JNT-9.

To accommodate the low capacitances of these probes, we also exchanged the transmission lines within the JJ probe to lower the capacitance and to match the impedance with the JNT probes.

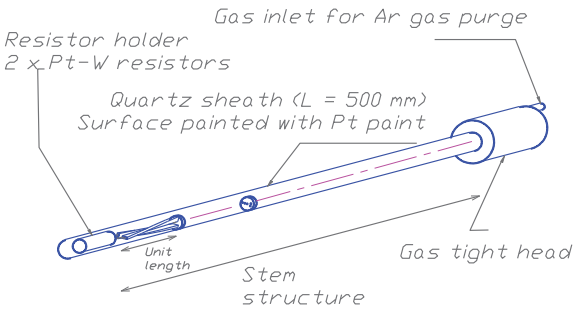


**FIGURE 1.** Structure of the JNT resistance probe.

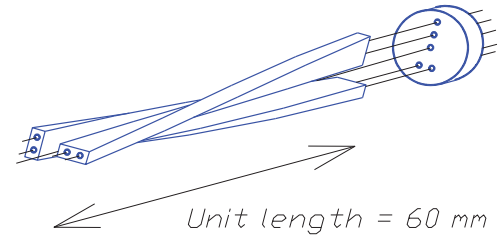


(a) JNT-9 Probe

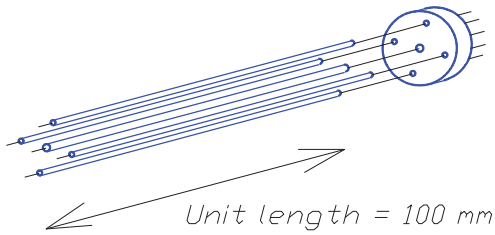


(b) JNT-10 Probe

**FIGURE 2.** Unit structure of probes JNT-9 and JNT-10.

## Amplifier System and Digitizer

The amplifier used in this work is an improved version from that used in our previous work [8]. It has a JFET input cascade for the differential input. The new version has a bias compensation aimed to reduce the amplitude dependent distortion within the circuit. Furthermore, in our present system, we added an 800 kHz low pass filter (LPF) in series to the existing 650 kHz LPF to further suppress the aliased signal from above our Nyquist frequency. The digitizers used are the same as the previous work, with the signal over sampled at 50 MHz sampling rate with 14 bits, and then down sampled to 2.09 MHz with 24 bits.

## QVNS noise patterns

The QVNS generates a pseudo-noise signal as the reference to measure the noise generated from the resistor within the JNT probe. The pseudo noise is synthesized via a delta-sigma modulation scheme using a bit stream generator with a sampling frequency $f_s$. The pseudo-noise signal is synchronized to the 10 MHz system master clock and the same waveform is repeated at a repetition rate $f_1 = f_s/M$, where $M$ is the bit pattern length. The synthesis produces a harmonic series of tones in the frequency domain with a fundamental tone $f_1$ [12].

For our previous work, we employed a single 6.293 Mbit waveform with $f_1$=1589 Hz and odd harmonics up to $f_{max}$=8 MHz. Using only one waveform can obscure the existence of a systematic error (e.g. due to distortion products) specific to that waveform. Furthermore, the order of the delta-sigma modulation, $N_{\Delta\Sigma}$, can change the unwanted out-of-band signal intensity [12]. Finer tone spacing is preferable to reduce spectral errors [8, 13]. The bit stream generator available in Gaithersburg is limited to bit patterns of $M$<8 Mbit. Since changing the bit stream generator clock frequency $f_s$ will also change both $f_1$ and the tone spacing of the harmonic series, as a first attempt in the Gaithersburg laboratory, we lowered the sampling clock to $f_s$=5 GHz to yield $f_1$=795 Hz fundamental frequency.

In our earlier runs in this work, we made measurements using the waveforms listed in Table 1. We use the notation $J_{odd}(N_{\Delta\Sigma}, f_{max})$ to indicate an odd harmonic waveform of delta-sigma order $N_{\Delta\Sigma}$ and maximum harmonic frequency $f_{max}$.

**TABLE 1.** The various waveforms used to drive the JJs as the reference in this work.

| Waveform | $N_{\Delta\Sigma}$ | $f_1$, $f_{max}$, $f_s$ |
|---|---|---|
| $J_{odd}(2,8)$ | 2nd | 1589 Hz, 8 MHz, 10 GHz |
| $J_{odd}(3,8)$ | 3rd | 1589 Hz, 8 MHz, 10 GHz |
| $J_{odd}(2,4)$ | 2nd | 795 Hz, 4 MHz, 5 GHz |
| $J_{odd}(3,4)$ | 3rd | 795 Hz, 4 MHz, 5 GHz |

*All waveforms use only odd harmonics of the fundamental.

## RESULTS

Figure 3 shows an example of the absolute mode ratio and the relative mode ratio obtained using the JNT10 probe. The noise waveform pattern used for the JJs was $J_{odd}(2, 8)$ with 1589 Hz fundamental frequency and 3198 Hz tone spacing. The absolute ratio plot (circles) shows the absolute ratio $\langle S'_R/S'_J \rangle$ for each frequency bin around the JJ tone peak. The black line is a quadratic fit of the data. As we can see in Fig. 4, the intercept of the absolute ratio at the low frequency limit $a_0 = \langle S'_R/S'_J \rangle|_{f=0}$ was approximately $10^{-4}$ higher than unity. This abnormal offset appeared for all the data in this work. Assuming that some distortion in the amplifier system is causing this large offset, we have

tested various modifications to the amplifiers and the transmission lines. Through such modifications, we succeeded in yielding a better match for the time constants between the JJ probe and the resistor probe; the quadratic roll off of the absolute spectral power ratio from 4.8 kHz to 600 kHz in our previous system was approximately 1 % at 693 K. This was improved to as small as 0.3% using JNT-9 probe and 0.25 % using the JNT-10 probe. Changing the pseudo-noise waveform pattern could also change the amount of distortion if it were dependent on the waveform. We tested the various waveforms listed in Table 1. However, there was not much difference in the offset level, and we also found that reducing the tone spacing results in a larger scatter in the binned ratio, and it does not contribute to improving the statistics in the measurements. Despite these efforts, the source of the offsets in the absolute ratio data remains unresolved.

Calculating the ratio in relative mode can remove the spectral aberration if the distortion product is common for measurements at two different temperatures when using the same waveform. The plot with red squares also shown in Fig. 3 is the relative ratio $\langle S'_{R2}/S'_{J2}\rangle/\langle S'_{R1}/S'_{J1}\rangle$ for 693 K and 505 K with JNT-10. As we can see in the plot, the spectral aberration is relaxed, and the residuals to the quadratic fit are more randomly distributed. Thus, for this work, we will present only the relative mode data for the $T$-$T_{90}$ measurements.

Figure 4 shows the results of $T$-$T_{90}$ from relative mode measured from the various runs using both JNT-9 and JNT-10 probes. The $T$-$T_{90}$ in Fig. 5 is corrected by the acoustic thermometry results [14] at 505K following the same correction method reported in [7].

For the JNT-10 probe, the $T$-$T_{90}$ results among different runs including the use of various pseudo-noise waveforms agreed well when considering the uncertainties of each measurement described in the next section. At 693 K, the results for both JNT-9 and JNT-10 probes are in reasonable agreement. However, for the JNT-9 probe at 730 K and above, the $T$-$T_{90}$ results are systematically low. We show in the next section how the JNT-9 probe is subject to systematic errors which are consistent with negative errors of the observed magnitude. Therefore, we only list the $T$-$T_{90}$ obtained data by JNT-10 probe as shown in Table 2.

## DISCUSSION

Tables 3 and 4 show the uncertainty of the measurements. The factors of uncertainty basically follow our previous work [7]. For the factors related to the furnace, we extrapolated the uncertainties from the knowledge up to 693 K. An additional term "Stability" was added as a type B term to Table 4 to represent the

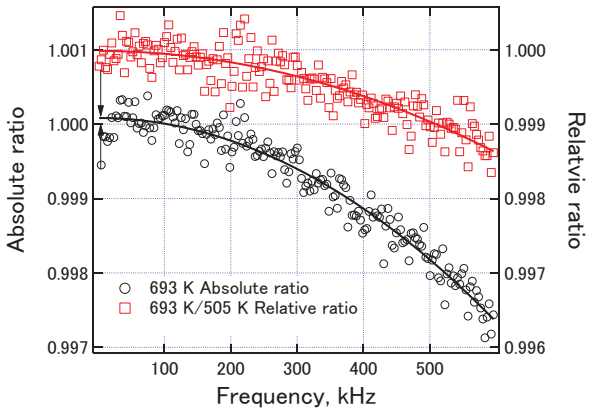


**FIGURE 3.** Absolute spectrum at 693 K (circles) and relative spectrum for the ratio between 693 K and 505 K (squares) of JNT-10 probe. The arrows show the large irresolvable offset from unity in the absolute spectra.

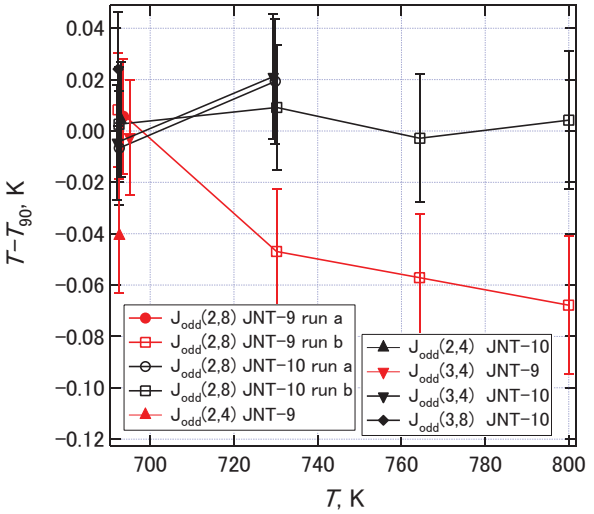


**FIGURE 4.** $T$-$T_{90}$ from relative mode measured from the various runs using JNT-9 and -10 probes with the various reference waveforms listed in Table 1. Error bars indicate the measurement uncertainties shown in Table 4.

**TABLE 2.** $T$-$T_{90}$ from relative mode measured from the various runs using JNT-10 probe. The statistical uncertainty $u_s$ is derived for the relative mode data.

| Temperature K | Pseudo-noise Waveform | $T$-$T_{90}$ ($u_s$) mK |
|---|---|---|
| 692.509 | $J_{odd}(2,4)$ | 4.4 (11.8) |
| 692.550 | $J_{odd}(2,8)$ | 2.6 (15.7) |
| 692.622 | $J_{odd}(2,8)$ | -6.6 (9.0) |
| 692.662 | $J_{odd}(3,4)$ | -4.4 (10.6) |
| 692.842 | $J_{odd}(3,4)$ | 24.1 (19.3) |
| 729.869 | $J_{odd}(2,8)$ | 19.3 (10.0) |
| 729.880 | $J_{odd}(3,4)$ | 21.2 (10.9) |
| 730.213 | $J_{odd}(2,8)$ | 9.2 (13.8) |
| 764.377 | $J_{odd}(2,8)$ | -2.8 (15.7) |
| 799.946 | $J_{odd}(2,8)$ | 4.2 (17.9) |

**TABLE 3.** Uncertainties for ITS-90 measurements (mK).

| | 505 K | 693 K | 730 K | 764 K | 800 K |
|---|---|---|---|---|---|
| Stability (A) | 0.7 | 1.5 | 4.8 | 2.6 | 2.1 |
| Immersion (B) | 1.0 | 2.0 | 2.2 | 2.4 | 2.6 |
| Non-uniformity (B) | 2.4 | 2.5 | 3.0 | 3.0 | 3.1 |
| Resistance measurement (B) | 0.3 | 0.3 | 0.3 | 0.3 | 0.3 |
| SPRT calibration (B) | 0.1 | 0.3 | 0.3 | 0.3 | 0.3 |
| RSS | 2.7 | 3.5 | 6.1 | 4.6 | 4.6 |

**TABLE 4.** Uncertainty for relative mode $T - T_{90}$ measurements using JNT-10 (in μK/K).

| | 693 K | 730 K | 764 K | 800 K |
|---|---|---|---|---|
| Statistics (A)† | 22.7 | 19.3 | 19.6 | 20.1 |
| Stability (B) | 17.3 | 17.3 | 17.3 | 17.3 |
| EMI (B) | 14.0 | 14.0 | 14.0 | 14.0 |
| QVNS (B) | 0.1 | 0.1 | 0.1 | 0.1 |
| Resistance (B) | 2.0 | 2.0 | 2.0 | 2.0 |
| Distortion (B) | 1.7 | 4.3 | 2.3 | 4.5 |
| RSS | 31.8 | 29.8 | 29.8 | 30.4 |
| ITS-90†† | 9.0 | 11.5 | 10.2 | 10.3 |
| Combined ($k$ = 1) | 33.2 | 32.0 | 31.5 | 32.1 |
| in mK | 23.0 | 23.3 | 24.1 | 25.7 |

†including the maximum value from measurements at each $T$.
††including both ITS-90 uncertainties at each temperature and the propagation of the ITS-90 uncertainties at 505 K.

instability of the amplifier distortion among various runs. Since the matching of the JNT and JJ probes has vastly improved and the fitting model is purely quadratic, we eliminated the uncertainty factor related to the choice of the fitting function. However, there are clear indications of distortion at lower frequencies. This increases the effective statistical uncertainty and introduces the possibility of distortion-induced offsets. The type B uncertainties are estimated from the difference in the fitting result to zero frequency $a_0$ when all tones were included and when tones below 50 kHz were excluded The combined uncertainties shown in Table 4 are in the range 23 mK to 26 mK ($k$=1), increasing at higher temperatures.

As shown in Fig. 4, the JNT-10 probe yielded results consistent with ITS-90 temperatures. However, the $T$-$T_{90}$ calculated for JNT-9 was systematically low for $T \geq 730$ K. The larger diameter of the stem structure and also the cross section of the insulators for JNT-9, compared to that of JNT-10, could in principle lead to negative immersion errors. However, these errors are well within the allowances for non-uniformity uncertainty given in Table 3. We therefore examine other possible causes for the difference.

We chose to dismount the resistor element from JNT-9 probe and assemble another probe without the resistor but with the same stem structure as used in JNT-10 to investigate leakage and loss effects within the insulators of the probes.

Measurements of DC leakage resistance were performed using bias voltages from -10 V to +10 V and allowing transient currents to settle for several minutes. We found that even though some rectifying effect does appear by changing the applied voltage, the resistance at 0 V bias remained above $10^9$ Ω for both probes for temperatures up to 800 K. The sigmoid feature reported in quartz insulators at higher temperatures [15] did not appear in these measurements.

Measurements of the AC impedances of the open-circuit probe stem of JNT-9, however, revealed a large dielectric loss peak at lower frequencies for JNT-9. The dielectric loss peak was temperature dependent with the frequency peak shifting to higher frequencies with increasing temperature as shown in Fig. 5.

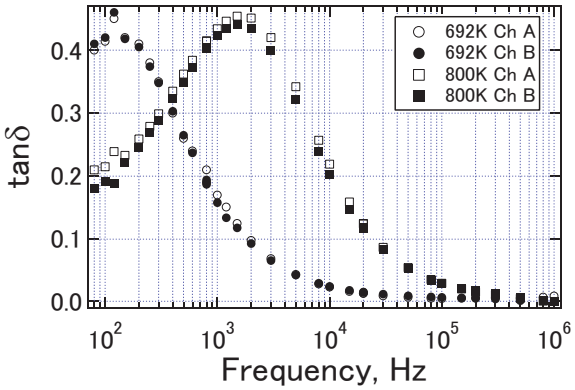


**FIGURE 5.** Loss tangent of the JNT-9 probe stem structure measured using a LCR meter. The uncertainty is ±10% + 0.0005 in loss tangent.

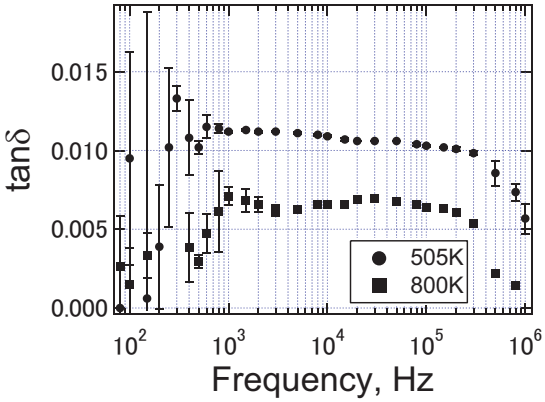


**FIGURE 6.** Loss tangent of the JNT-10 probe stem structure measured using a LCR meter.

In contrast, as shown in Fig. 6, the loss tangent was remarkably small and relatively flat in frequency for the JNT-10 probe stem. The AC measurements were accomplished using a four-terminal-pair LCR meter from 100 Hz to 1 MHz.

When some dielectric loss $\delta$ exists in a capacitance $C$ at temperature $T_C$ in the stem as shown in Fig. 7, the noise observed at both amplifiers will be

$$v^2 \cong 4kTR\left[(1-4\omega RC\tan\delta)+\frac{T_C}{T}\cdot 2\omega RC\tan\delta\right], \quad (5)$$

where both $\delta$ and $C$ are frequency dependent. The first term represents the attenuation of the resistor noise due to the filtering effect from an effective shunt conductance $G_C = 2\omega C\tan\delta$ . This term remains negative for all realistic conditions. The second term is the noise generated by the shunt conductance itself, attenuated by the sense resistor $R$. For $T_C$~$T$, the net effect is a frequency dependent negative error.

As shown in Fig. 5, the loss tangent for JNT-9 is both frequency dependent and temperature dependent. As temperature is increased more of the loss peak appears within our measurement band. The combined frequency dependence of the product $\omega C(\omega)\tan\delta(\omega)$ creates a negative shift to the fit parameter $a_0$ for all JNT-9 ratio spectra and this is most pronounced at 800 K. In the case of the JNT-10, however, the magnitude of both $C$ and $\tan\delta$ are significantly smaller, so the expected effect would be a small negative linear frequency error term according to Eqn. 5. The existence of such a small linear error in the JNT-10 spectra would be expected to shift the fitted $a_0$ parameter by less than 1 μK/K. It is possible that the effect is vastly reduced for JNT-10 due to smaller cross sections of the insulators compared to those used in JNT-9.

Upon consideration of the above-mentioned results, we choose to present only JNT-10 probe data in Table 2. More consideration of the insulating materials and their effect on the measurement results is needed for further improvements.

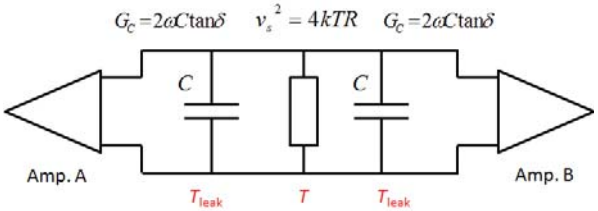


**FIGURE 7.** Noise model when a lossy insulator with a shunt conductance $G_C$ is placed at temperature $T_{leak}$.

## Summary

We modified the JNT system for $T$–$T_{90}$ measurements at 505 K – 800 K. For the probes, we reduced the capacitance on the transmission lines, yielding a better matching of time constants and a flatter ratio spectrum. For the amplification system and the QVNS operation, we followed some aspects presented in refs. 8 and 13. Employing the modified system, we performed $T$–$T_{90}$ measurements up to 800 K with two new probes. The results are listed in Table 2. Since the amplifying system had more distortion than expected, showing an irresolvable high offset in the absolute spectra, all the $T$–$T_{90}$ data presented here was obtained from relative mode, with correction to acoustic data at 505 K made as described in ref. 7). The data using the probe JNT-10 had $T$–$T_{90}$ results consistent with those obtained from other methods.

The use of amplifiers and digitizers with lower distortion, further matching of the probes and more consideration of the behavior of insulating materials will be the keys to improving future measurements.

## ACKNOWLEDGEMENTS

We thank D.R. White (MSL, IRL) and J.F. Qu (NIM) for valuable discussions. M. Chojnacky provided the ITS-90 calibration and others such as G. Strouse, C. Urano, J. Tamba and N. Kaneko provided assistance. This collaboration was supported by the NIST Temperature and Humidity Group and the JSPS Institutional Program for Young Researcher Overseas Visits. The amplifiers were funded by Grant-in-Aid for Scientific Research (KAKENHI) project (A) 22246013.

## REFERENCES

1. http://www.bipm.org/en/CGPM/db/24/1/
2. CCT/10-15/rev2
3. Fischer, J., *et al*., *Int. J. Thermophys.* **32**, pp. 12–25 (2011).
4. Labenski, J. R., *et al*., *IEEE Trans. Instr. Meas.* **58**, pp. 481-485 (2007).
5. Tew, W. L., *et al*., *Int. J. Thermophys.* **28**, pp. 629–645 (2007).
6. Labenski *et al*., *Int. J. Thermophys.* **29**, pp. 1─17 (2008).
7. Tew *et al*., *Int. J. Thermophys.* **31**, pp. 1719–1738 (2010).
8. Qu, J. *et al*., *Metrologia*, **46**, pp.521–524 (2009).
9. Johnson J. B., *Phys. Rev. Lett.* **32**, 97-109 (1928).
10. Nyquist H., *Phys. Rev. Lett.* **32**, 110-113 (1928).
11. Benz, S. P., *et al*., *IEEE Trans. Instr. Meas.* **58**, pp. 884–890 (2009).
12. Benz, S. P., Dresselhaus, P., and Burroughs, C., *IEEE Trans. Appl. Supercond.* **21**, pp. 681–686 (2011).
13. Qu, J., *et al., IEEE Trans. Instr. Meas.* **60**, pp. 2427-2433 (2011).
14. Strouse et al., in *Temperature: Its Measurement and Control in Science and Industry* **7**, pp. 31–36 (2003).
15. Yamazawa et al., *Int. J. Thermophys.* **28**, pp. 1855-67 (2007).